Geochemical Perspectives Letters

Crustal controls on isotope variability of light noble gases along the Andean Volcanic Arc

J. Lages, A.L. Rizzo, A. Aiuppa, P. Robidoux, R. Aguilar, F. Apaza, P. Masias

Supplementary Information

The Supplementary Information includes:

S-1 New Isotope Results and Noble Gas Abundances (Peru and S Chile)

Brief Petrological Descriptions of Volcanoes Sampled in This Study

Sabancaya (Peru, CVZ)

The Ampato–Sabancaya volcanic complex comprises two successive edifices. During the Holocene, eruptive activity migrated to the NE and built up the Sabancaya edifice, between 6 and 3 ka. This cone comprises andesitic and dacitic blocky lava flows emplaced during at least two eruptive stages (Samaniego *et al*., 2016). The Ampato–Sabancaya rocks display a high-K magmatic affinity and range from andesites to dacites (57–69 wt. % SiO_2), with rare rhyolitic compositions (74–77 wt. % SiO_2). We analysed two lava samples from the Sabancaya basal edifice (3 ± 5 ka; Samaniego *et al*., 2016) that present porphyritic texture, composed of phenocrysts (30–60 vol. %) of plagioclase, biotite, amphibole, clinopyroxene, Fe-Ti oxides, and eventually by orthopyroxene and olivine (<2 %; Samaniego *et al*., 2016). The FIs analysed from noble gases in this study were entrapped in clinopyroxene host minerals (Table S-1).

Ubinas (Peru, CVZ)

Over the past 500 years, Ubinas produced mostly tephra with a trend towards more mafic magma compositions in recent times (Thouret *et al*., 2005). The 2006 and 2014 juvenile blocks here analysed are dark to grey, dense to poorly vesicular, porphyritic andesites bearing 20–25 vol. % phenocrysts (300 µm to 1.8 mm), 30–40 vol. % microphenocrysts (100–300 µm), and 35–50 vol. % matrix glass. Phenocrysts of plagioclase, clinopyroxene, orthopyroxene, and Fe-Ti oxides are abundant. Both samples show a similar mineral assemblage including plagioclase, clinopyroxene, orthopyroxene, and magnetite with scarce amphibole and olivine (Rivera *et al*., 2014). Olivine phenocrysts occur in the 2006 ballistic blocks, although not in sufficient amounts for FIs analysis of noble gases.

El Misti (Peru, CVZ)

El Misti is a major andesitic volcano located near the city of Arequipa in the northern Central Volcanic Zone. Plagioclase is by far the most abundant mineral phase followed in order of abundance by amphibole and pyroxene. Olivine occurs only in mafic andesites and when present is scarce, never exceeding 2 vol. %. Rivera *et al*. (2017) report on subhedral to anhedral olivine crystals with sizes smaller than 400 µm for Misti 2 lava flows from which both samples in this study were collected (112–40 ka), with forsterite composition of $Fo_{76–80}$. When compared with olivines from primitive arc magmas (Fo_{80}), the relatively low-Fo content of the El Misti olivine ($Fo_{70–80}$) provides evidence against a pure, primary, mantled-derived origin for El Misti rocks (Rivera *et al*., 2017).

Villarrica (CSVZ, South Chile)

Activity at Villarrica has been characterised in the past by frequent small eruptions as well as highly explosive, caldera-forming pyroclastic eruptions of mainly basaltic andesite magma (Moreno and Clavero, 2006). Samples collected for analysis included scoria samples from the 3 March 2015 paroxysmal eruption (Aiuppa *et al*., 2017), with Fo contents ranging from about 70 to 82 % (avg. 77 %). Previously analysed samples representing the magma filling the central crater were determined to hold 33 wt. % plagioclase ($An_{58–74}$), 7 wt. % olivine ($Fo_{75–78}$), and trace amounts of chromian spinel (Witter *et al*., 2004). The other sample analysed (HCH2A1; Sancho, 2019) is taken from a ~100-m-high adventitious eruptive centre from the sub-group 2 of Chaillupén hch2 (<3.7 ka; Moreno and Clavero, 2006). The rock represents a ballistic projectile taken on the crater rim of a pyroclastic cone, ubicated downhill at the southern end of the N–S fracture that cuts through Villarrica's south flank. The rock sample is characterised as a fine-grained, dense fusiform bomb-size pyroclast of mafic composition with 20 vol. % plagioclase, 6 vol. % clinopyroxene, 4 vol. % olivine as determined from thin section analysis.

Table S-1 Noble gas abundances and isotope compositions in fluid inclusions (Peru and S Chile).

Volcano	Sample ID	Sample details	Rock[a]	Min. phase[b]	[He][c] $\times10^{-13}$	[Ne][c] $\times10^{-17}$	[^{40}Ar][c] $\times10^{-12}$	[^{36}Ar][c] $\times10^{-15}$	[^{40}Ar*][c] $\times10^{-13}$	^{4}He/^{20}Ne	^{20}Ne/^{22}Ne	^{21}Ne/^{22}Ne	^{4}He/^{40}Ar*	^{40}Ar/^{36}Ar	^{3}He/^{4}He (R/R$_A$)	^{3}He/^{4}He (R$_C$/R$_A$)	CO_2/^{3}He[c] $\times10^{-9}$
South Chile (SVZ)																	
Villarrica	2015_B	Scoria	BA	Ol	1.27	2.50	6.15	20.38	1.24	50.8	9.83 ± 0.03	0.0295 ± 0.0005	1.02	301.6 ± 0.1	6.43	6.46 ± 0.12	0.013
	HCH2A1	Pyroclast (bomb)	BA	Ol	0.72	10.32	1.03	3.40	0.21	7.0	9.81 ± 0.02	0.0293 ± 0.0003	3.39	301.8 ± 0.7	6.39	6.66 ± 0.13	0.627
Peru (CVZ)																	
Ubinas	2014	Juvenile blocks	A	Cpx	0.72	9.86	6.95	19.75	11.19	7.3	9.67 ± 0.02	0.0284 ± 0.0003	0.06	352.2 ± 0.8	5.64	5.86 ± 0.16	16.461
	2016 A & B	Juvenile blocks	A	Cpx	1.29	39.69	15.27	48.72	8.75	3.2	9.66 ± 0.02	0.0285 ± 0.0002	0.15	313.5 ± 0.04	5.49	6.01 ± 0.16	7.203
Sabancaya	SA-09-11	Lava flow	A	Cpx	0.38	10.63	0.71	1.98	1.27	3.6	9.67 ± 0.03	0.0288 ± 0.0004	0.30	359.7 ± 0.2	5.45	5.92 ± 0.23	0.484
	SA-09-17	Lava flow	A	Cpx	0.08	12.57	0.93	2.92	0.70	0.7	9.77 ± 0.01	0.0292 ± 0.0003	0.12	319.4 ± 0.1	1.45	2.11 ± 0.18	16.460
El Misti	Misti 2 (A)	Lava flow	A	Cpx	1.19	2.18	4.16	1.35	1.82	0.9	9.89 ± 0.01	0.0289 ± 0.00031	0.08	309.0 ± 0.06	3.93	5.80 ± 0.177	–
	Misti 2 (B)	Lava flow	A	Cpx	0.78	1.31	4.84	1.56	2.32	0.9	9.84 ± 0.01	0.0297 ± 0.00019	0.12	310.4 ± 0.06	4.43	6.36 ± 0.190	–

[a] Host rock chemical classification on the basis of SiO_2 content: A, andesite; BA, basaltic-andesite.

[b] Mineral phases analysed: Ol, olivine; Cpx, clinopyroxene.

[c] Noble gas and CO_2 concentrations in mol g^{-1}.

S-2 Data References, Dataset Description, and Full Data Table (with Table Guide)

The data table below includes He, Ar, and Ne data available for quaternary volcanoes from the Andean Volcanic Arc. Noble gas data reported for amagmatic regions of the arc (*e.g.*, flat-slab segments) have not been included (see Simmons *et al*., 1987; Hoke *et al*., 1994; Hoke and Lamb, 2007; Newell *et al*., 2015).

S-2.1 Catalogue References (in Table S-2)

1. Williams, S.N., Sano, Y., Wakita, H. (1987) Helium-3 emission from Nevado Del Ruiz Volcano, Colombia. *Geophysical Research Letters* 10, 1035–1038.

2. Sano, Y., Wakita, H., Williams, S.N. (1990) Helium-isotope systematics at Nevado del Ruiz volcano, Colombia: implications for the volcanic hydrothermal system. *Journal of Volcanology and Geothermal Research* 42, 41–52.

3. Lages, J., Rizzo, A.L., Aiuppa, A., Samaniego, P., Le Pennec, J.L., Ceballos, J.A., Narváez, P.A., Moussallam, Y., Bani, P., Schipper, C.I., Hidalgo, S., Gaglio, V., Alberti, E., Sandoval-Velasquez, A. (2021) Noble gas magmatic signature of the Andean Northern Volcanic Zone from fluid inclusions in minerals. *Chemical Geology* 559, 119966.

4. Sturchio, N.C., Williams, S.N., Sano, Y. (1993) The hydrothermal system of Volcan Puracé, Colombia. *Bulletin of Volcanology* 55, 289–296.

5. Maldonado, L.F.M., Inguaggiato, S., Jaramillo, M.T., Valencia, G.G., Mazot, A. (2017) Volatiles and energy released by Puracé volcano. *Bulletin of Volcanology* 79, 84.

6. Sano, Y., Williams, S.N. (1996) Fluxes of mantle and subducted carbon along convergent plate boundaries. *Geophysical Research Letters* 23, 2749–2752.

7. Sano, Y., Gamo, T., Williams, S.N. (1997) Secular variations of helium and carbon isotopes at Galeras volcano, Colombia. *Journal of Volcanology and Geothermal Research* 77, 255–265.

8. Inguaggiato, S., Londoño, J.M., Chacón, Z., Liotta, M., Gil, E., Alzate, D. (2017) The hydrothermal system of Cerro Machín volcano (Colombia): New magmatic signals observed during 2011–2013. *Chemical Geology* 469, 60–68.

9. Lewicki, J.L., Fischer, T., Williams, S.N. (2000) Chemical and isotopic compositions of fluids at Cumbal Volcano, Colombia: Evidence for magmatic contribution. *Bulletin of Volcanology* 62, 347–361.

10. Fischer, T.P., Sturchio, N.C., Stix, J., Arehart, G.B., Counce, D., Williams, S.N. (1997) The chemical and isotopic composition of fumarolic gases and spring discharges from Galeras Volcano, Colombia. *Journal of Volcanology and Geothermal Research* 77, 229–253.

11. Inguaggiato, S., Hidalgo, S., Beate, B., Bourquin, J. (2010) Geochemical and isotopic characterization of volcanic and geothermal fluids discharged from the Ecuadorian volcanic arc. *Geofluids* 10, 525–541.

12. Hilton, D.R., Hammerschmidt, K., Teufel, S., Friedrichsen, H. (1993) Helium isotope characteristics of Andean geothermal fluids and lavas. *Earth and Planetary Science Letters* 120, 265–282.

13. Inostroza, M., Tassi, F., Aguilera, F., Sepúlveda, J.P., Capecchiacci, F., Venturi, S., Capasso, G., 2020. Geochemistry of gas and water discharge from the magmatic-hydrothermal system of Guallatiri volcano, northern Chile. *Bulletin of Volcanology* 82, 57.

14. Lopez, T., Aguilera, F., Tassi, F., Maarten de Moor, J., Bobrowski, N., Aiuppa, A., Tamburello, G., Rizzo, A.L., Liuzzo, M., Viveiros, F., Cardellini, C., Silva, C., Fischer, T., Jean-Baptiste, P., Kazayaha, R., Hidalgo, S., Malowany, K., Lucic, G., Bagnato, E., Bergsson, B., Reath, K., Liotta, M., Carn, S., Chiodini, G. (2018) New insights into the magmatic-hydrothermal system and volatile budget of Lastarria volcano, Chile: Integrated results from the 2014 IAVCEI CCVG 12th Volcanic Gas Workshop. *Geosphere* 14, 983–1007.

15. Aguilera, F., Tassi, F., Darrah, T., Moune, S., Vaselli, O. (2012) Geochemical model of a magmatic-hydrothermal system at the Lastarria volcano, northern Chile. *Bulletin of Volcanology* 74, 119–134.

16. Tassi, F., Aguilera, F., Vaselli, O., Medina, E., Tedesco, D., Delgado Huertas, A., Poreda, R., Kojima, S. (2009) The magmatic- and hydrothermal-dominated fumarolic system at the Active Crater of Lascar volcano, northern Chile. *Bulletin of Volcanology* 71, 171–183.

17. Tassi, F., Aguilera, F., Vaselli, O., Darrah, T., Medina, E. (2011) Gas discharges from four remote volcanoes in northern Chile (Putana,Olca, Irruputuncu and Alitar): A geochemical survey. *Annals of Geophysics* 54, 121–136.

18. Roulleau, E., Tardani, D., Sano, Y., Takahata, N., Vinet, N., Bravo, F., Muñoz, C., Sanchez, J. (2016) New insight from noble gas and stable isotopes of geothermal/hydrothermal fluids at Caviahue-Copahue Volcanic Complex: Boiling steam separation and water-rock nteraction at shallow depth. *Journal of Volcanology and Geothermal Research* 328, 70–83.

19. Tassi, F., Aguilera, F., Benavente, O., Paonita, A., Chiodini, G., Caliro, S., Agusto, M., Gutierrez, F., Capaccioni, B., Vaselli, O., Caselli, A., Saltori, O. (2016) Geochemistry of fluid discharges from Peteroa volcano (Argentina-Chile) in 2010–2015: Insights into compositional changes related to the fluid source region(s). *Chemical Geology* 432, 41–53.

20. Agusto, M., Tassi, F., Caselli, A.T., Vaselli, O., Rouwet, D., Capaccioni, B., Caliro, S., Chiodini, G., Darrah, T. (2013) Gas geochemistry of the magmatic-hydrothermal fluid reservoir in the Copahue-Caviahue Volcanic Complex (Argentina). *Journal of Volcanology and Geothermal Research* 257, 44–56.

21. Robidoux, P., Rizzo, A.L., Aguilera, F., Aiuppa, A., Artale, M., Liuzzo, M., Nazzari, M., Zummo, F. (2020) Petrological and noble gas features of Lascar and Lastarria volcanoes (Chile): Inferences on plumbing systems and mantle characteristics. *Lithos* 370–371, 105615.

22. Benavente, O., Tassi, F., Reich, M., Aguilera, F., Capecchiacci, F., Gutiérrez, F., Vaselli, O., Rizzo, A. (2016) Chemical and isotopic features of cold and thermal fluids discharged in the Southern Volcanic Zone between 32.5°S and 36°S: Insights into the physical and chemical processes controlling fluid geochemistry in geothermal systems of Central Chile. *Chemical Geology* 420, 97–113.

23. Ray, M.C., Hilton, D.R., Muñoz, J., Fischer, T.P., Shaw, A.M. (2009) The effects of volatile recycling, degassing and crustal contamination on the helium and carbon geochemistry of hydrothermal fluids from the Southern Volcanic Zone of Chile. *Chemical Geology* 266, 38–49.

24. Tardani, D., Reich, M., Roulleau, E., Takahata, N., Sano, Y., Pérez-Flores, P., Sánchez-Alfaro, P., Cembrano, J., Arancibia, G. (2016) Exploring the structural controls on helium, nitrogen and carbon isotope signatures in hydrothermal fluids along an intra-arc fault system. *Geochimica et Cosmochimica Acta* 184, 193–211.

25. Capaccioni, B., Aguilera, F., Tassi, F., Darrah, T., Poreda, R.J., Vaselli, O. (2011) Geochemical and isotopic evidences of magmatic inputs in the hydrothermal reservoir feeding the fumarolic discharges of Tacora volcano (northern Chile). *Journal of Volcanology and Geothermal Research* 208, 77–85.

26. Benavente, O., Tassi, F., Gutiérrez, F., Vaselli, O., Aguilera, F., Reich, M. (2013) Origin of fumarolic fluids from Tupungatito Volcano (Central Chile): Interplay between magmatic, hydrothermal, and shallow meteoric sources. *Bulletin of Volcanology* 75, 1–15.

27. Hoke, L., Hilton, D.R., Lamb, S.H., Hammerschmidt, K., Friedrichsen, H. (1994) ^{3}He evidence for a wide zone of active mantle melting beneath the Central Andes. *Earth and Planetary Science Letters* 128, 341–355.

28. Tassi, F., Aguilera, F., Darrah, T., Vaselli, O., Capaccioni, B., Poreda, R.J., Delgado Huertas, A. (2010) Fluid geochemistry of hydrothermal systems in the Arica-Parinacota, Tarapacá and Antofagasta regions (northern Chile). *Journal of Volcanology and Geothermal Research* 192, 1–15.

S-2.2 Table Guidelines

The colours of the headlines throughout the noble gas catalogue table correspond to the colour scheme used in the figures to distinguish between the five different countries and their respective volcanic arc segments (NVZ, Colombia and Ecuador; CVZ, Peru and North Chile; SVZ, South Chile):

i) Lat and Long columns: "Lat" (latitude) and "Long" (longitude), when not provided, were estimated by name of sampling location and/or map figures showing sampling coordinates; values inferred appear in red in both columns. Note that FIs data are assigned the exact coordinates of the volcanic edifice of origin.

ii) Dist. (m) and Temp. (°C): Values for distance (Dist.) and temperature (Temp.), when not originally reported, were assigned based on sampling coordinates (for distance to the main volcanic centre) and previous temperatures reported for the same sampling location (for the temperature column), all in red. Samples with no temperature and/or distance information are due to insufficient information available to infer the sampling parameters. For hydrothermal samples not associated with a main volcanic system, the distance parameter results non-applicable (n/a).

iii) Type: The dataset is subdivided into the following sample types (see also Fig. 1 in the main text): 1, fluid inclusions (FIs) data in olivine phenocrysts; 2, FIs in clinopyroxene; 3, FIs in orthopyroxene; 4, free gases at >100 °C; 5, free gases at 50–100 °C; 6, free gases at <50 °C.

iv) Isotope ratios correction: Helium isotopic ratios reported in the form of R_C/R_A, where R_C is the air-corrected $^3He/^4He$ ratio of the sample, assessed based on $^4He/^{20}Ne$ ratios (also in table):

$$R_C/R_A = [(R_M/R_A)(He/Ne)_M - (He/Ne)_{air}]/[(He/Ne)_M - (He/Ne)_{air}],$$

where the subscripts "M" and "air" refer to measured and atmospheric theoretical values, respectively. Argon isotope ratios account for atmospheric-corrected ^{40}Ar, assuming that all ^{36}Ar contained in the gas phase is of atmospheric origin:

$$^{40}Ar^* = {}^{40}Ar_M - [(^{40}Ar/^{36}Ar)_{air} \times {}^{36}Ar_M],$$

where $^{40}Ar^*$ represents the corrected isotope value and M indicates the measured value.

v) err: Isotopic ratio errors are 1σ uncertainties.

Table S-2 Noble gas catalogue of the Andean Volcanic Arc.

Table S-2 is available for download (Excel) from the online version of the article at http://www.geochemicalperspectivesletters.org/article2134.

S-3 Neon and Argon Systematics of Andean Magmatic Fluids

In contrast to the extensive $^{3}He/^{4}He$ database described in the main text, there are relatively few $^{40}Ar/^{36}Ar$ samples (118) and even fewer $^{20}Ne/^{22}Ne$ and $^{21}Ne/^{22}Ne$ samples (34 and 33, respectively; Fig. S-1).

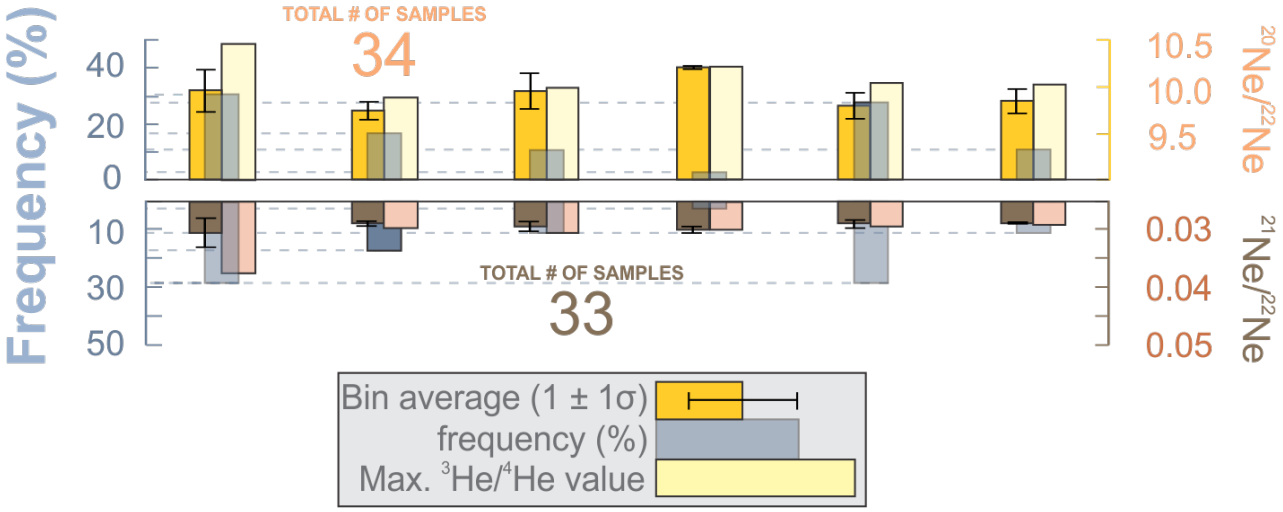

Figure S-1 Histogram of distribution, following those of Fig. 1 in the main text. Frequencies of the data type are shown on the left axis (faded columns; see Fig.1 in the main text for labels); averages (darker) and maximum values, per category, showed on the right axis.

Compared to intraplate and middle oceanic ridge environments, subduction-related fluids are known to carry larger proportions of atmospheric components (Burnard *et al*., 1997), and Ar isotopes in FIs from volcanic arc rocks consistently show $^{40}Ar/^{36}Ar$ ratios close to the atmosphere (295.5; Hilton *et al*., 2002). In our catalogue, the observed Andean gas-rocks $^{40}Ar/^{36}Ar$ ratios range from 287.5 to 610, but the arc average of ~339 (taken across all gas-rocks samples) denotes a close-to-atmospheric $^{40}Ar/^{36}Ar$ signature, well below that of MORB (~44,000; Moreira *et al*., 1998). Similarly, neon isotopes (≤0.038 for $^{21}Ne/^{22}Ne$ and ≤10.46 for $^{20}Ne/^{22}Ne$) cluster at around the atmospheric ratios (0.029 and 9.8 for $^{21}Ne/^{22}Ne$ and $^{20}Ne/^{22}Ne$, respectively; Sarda *et al*., 1988). These atmospheric Ar-Ne isotopic signatures imply variable (but substantial) degrees of contamination by an atmosphere-derived component that reflect their relatively large (compared to helium) air abundances (Hilton *et al*., 2002; Fig. S-2). Notably, FIs also exhibit this atmospheric imprint: their Ne isotopic pairs and $^{40}Ar/^{36}Ar$ ratios (see histogram in Figs. 1 and S-1) are often lower than in high-temperature gases and comparable to those obtained from low-temperature emission sources. Recycling of atmosphere-derived Ar in the mantle, via dehydration of the subducting oceanic crust, has often been invoked (Matsumoto *et al*., 2001; Hopp and Ionov, 2011; Di Piazza *et al*., 2015; Rizzo *et al*., 2016; Robidoux *et al*., 2017, 2020; Battaglia *et al*., 2018), although air contamination during surface rock exposure is often difficult to rule out.

Figure S-2 illustrates the binary trends of atmosphere-mantle mixing for both Argon and Neon isotopic ratios. Most importantly, our dataset indicates that atmosphere-derived components are still dominant even in FIs. Contrarily to the $^{3}He/^{4}He$ results, these show little difference when compared to argon and neon isotope results obtained in free gases, including those <100 °C (see Fig. 1 in the main text).

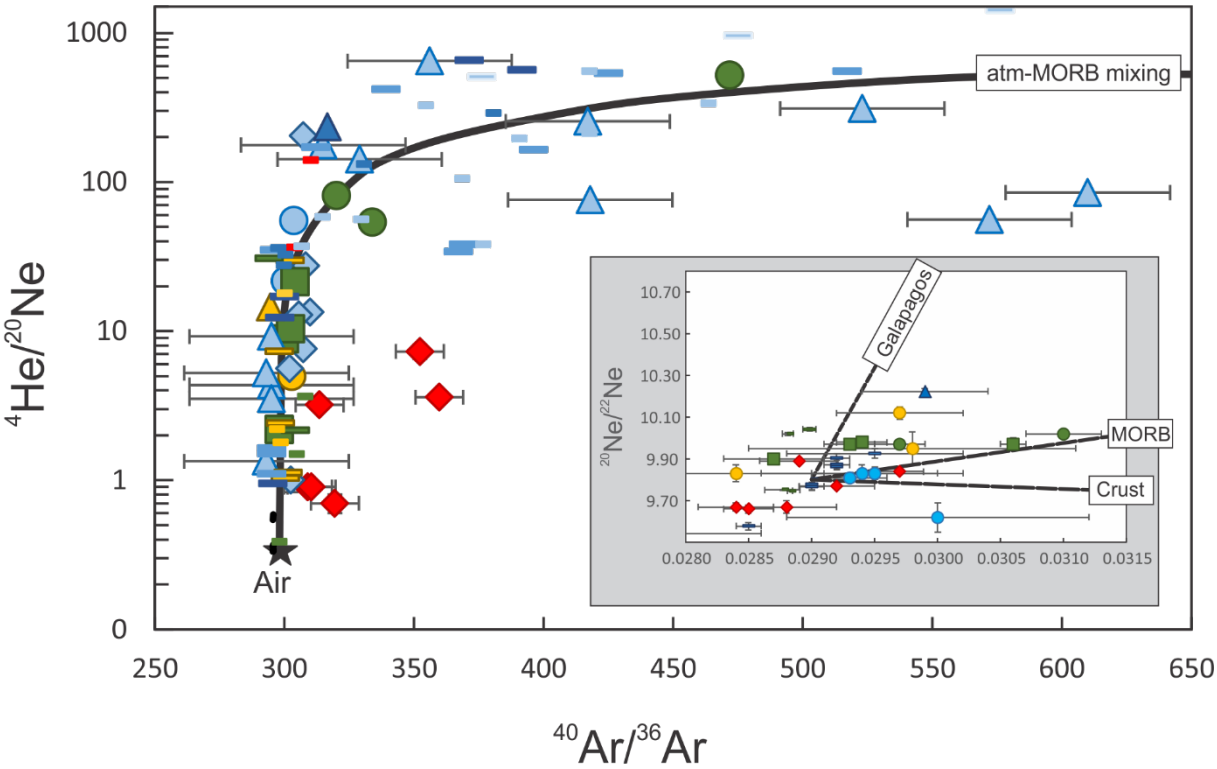

Figure S-2 Air-MORB mixing showing the extent of air contamination in samples from all categories (from FIs to low-temperature free gases); Inset: binary mixing between air and a MORB mantle as defined by Sarda *et al.* (1988) and Moreira *et al.* (1998) at $^{21}Ne/^{22}Ne$ = 0.06 and $^{20}Ne/^{22}Ne$ = 12.5; binary mixing between air and the OIB domain of the Galapagos Islands as determined by Kurz *et al.* (2009) at $^{21}Ne/^{22}Ne$ = 0.032 and $^{20}Ne/^{22}Ne$ = 12.5; crustal-neon trend from Kennedy *et al.* (1990).

S-4 Slab Constraints from Th/La in Sediments (Subducted) and Volcanic Products (Erupted) Along the Andean Volcanic Arc

To test the possible slab control on the $^{3}He/^{4}He$ signature of the mantle wedge along the Andes, we followed the approach of Plank (2005), who used the Th/La ratio as a tracer for the contribution of subducting sediments to arc magmas. This tracer is particularly useful since radiogenic ^{4}He mostly derives from the decay of natural U and Th series elements in rocks and sediments.

The author suggests that where little sediment subducts, arcs should have approximately mantle Th/La, whereas, in places with a high flux of subducted sediment, the Th/La of the arc should approach the sediment ratio. The latter varies with the proportions of terrigenous, hydrogenous and volcaniclastic sources. Th/La signatures in arc magmas should therefore provide information on the proportion of sediment to mantle, and therefore a way to calibrate the influence of sediment melts delivered by the slab at an arc-segment scale.

The Th/La data used in Figure 3a, b (main text) have been extracted from the 'GEOROC' (Geochemistry of Rocks of the Oceans and Continents) database (http://georoc.mpch-mainz.gwdg.de/georoc/Start.asp). The relevant data have been taken from the *'Precompiled Files/Locations/Convergent Margins'* files *'ANDEAN ARC part1.csv'* and *'ANDEAN ARC part2.csv'* that are freely available for download. The following tables summarise the available dataset.

Table S-3 Th/La data used in Figure 3a.

Volcanic products (GEOROC)			Sediments (Plank, 2014)		
Arc Segment	Bulk Arc Segment Th/La (avg.)*	1σ	Th/La	Th [ppm]	La [ppm]
Colombia	0.1007	0.0383	[1]0.083	1.21	14.6
Ecuador	0.1746	0.0464	[2]0.083	1.21	14.6
Peru	0.1723	0.1084	0.124	3.54	28.6
N Chile	0.2399	0.1133	0.332	5.08	15.3
S Chile	0.2177	0.1081	0.318	4.74	14.9

* Including only samples with <58 wt. % SiO_2.

[1,2] Th and La contents in sediments are averages for Colombia and Ecuador.

Table S-4 Th/La data used in Figure 3b.

GEOROC dataset				This review
Volcanic system	Avg Th/La of volcanic products	1σ	*N* samples	Maximum R_C/R_A
Nevado del Ruiz	0.2665	0.0798	4	8.46
Galeras	0.2953	0.0684	13	8.84
Cotopaxi	0.3099	0.1552	84	7.04
Tungurahua	0.3262	0.1183	89	7.40
El Reventador	0.1584	0.0182	15	6.98
Ubinas	0.1800	0.0344	14	6.01
El Misti	0.3462	0.2109	40	6.36
Sabancaya	0.2432	0.1303	14	5.92
Lascar	0.3160	0.1087	8	7.30
Lastarria	0.5908	0.1473	3	8.01
Villarica	0.1956	0.0694	10	6.66
Copahue	0.4165	0.0001	2	7.94

Supplementary Information References

Aiuppa, A., Bitetto, M., Francofonte, V., Velasquez, G., Parra, C.B., Giudice, G., Liuzzo, M., Moretti, R., Moussallam, Y., Peters, N., Tamburello, G., Valderrama, O.A., Curtis, A. (2017) A CO_2-gas precursor to the March 2015 Villarrica volcano eruption. *Geochemistry, Geophysics, Geosystems* 18, 2120–2132.

Battaglia, A., Bitetto, M., Aiuppa, A., Rizzo, A.L., Chigna, G., Watson, I.M., D'Aleo, R., Juárez Cacao, F.J., de Moor, M.J. (2018) The Magmatic Gas Signature of Pacaya Volcano, With Implications for the Volcanic CO_2 Flux from Guatemala. *Geochemistry, Geophysics, Geosystems* 19, 667–692.

Burnard, P., Graham, D., Turner, G. (1997) Vesicle-specific noble gas analyses of "popping rock": Implications for primordial noble gases in earth. *Science* 276, 568–571.

Di Piazza, A., Rizzo, A.L., Barberi, F., Carapezza, M.L., De Astis, G., Romano, C., Sortino, F. (2015) Geochemistry of the mantle source and magma feeding system beneath Turrialba volcano, Costa Rica. *Lithos* 232, 319–335.

Hilton, D.R., Fischer, T.P., Marty, B. (2002) Noble gases and volatile recycling at subduction zones. *Reviews in Mineralogy and Geochemistry* 47, 319–370.

Hoke, L., Lamb, S. (2007) Cenozoic behind-arc volcanism in the Bolivian Andes, South America: implications for mantle-melt generation and lithospheric structure. *Journal of the Geological Society* 164, 795–814.

Hoke, L., Hilton, D.R., Lamb, S.H., Hammerschmidt, K., Friedrichsen, H. (1994) ^{3}He evidence for a wide zone of active mantle melting beneath the Central Andes: *Earth and Planetary Science Letters*, 128, 341–355.

Hopp, J., Ionov. D.A. (2011) Tracing partial melting and subduction-related metasomatism in the Kamchatkan mantle wedge using noble gas compositions. *Earth and Planetary Science Letters* 302, 121–131.

Kennedy, B.M., Hiyagon, H., Reynolds, J.H. (1990) Crustal neon: a striking uniformity. *Earth and Planetary Science Letters* 98, 277–286.

Kurz, M.D., Curtice, J., Fornari, D., Geist, D., Moreira, M. (2009) Primitive neon from the center of the Galápagos hotspot. *Earth and Planetary Science Letters* 286, 23–34.

Matsumoto, T., Chen, Y.L., Matsuda, J. (2001) Concomitant occurrence of primordial and recycled noble gases in the Earth's mantle. *Earth and Planetary Science Letters* 185, 35–47.

Moreira, M., Kunz, J., Allègre, C. (1998) Rare gas systematics in popping rock: Isotopic and elemental compositions in the upper mantle. *Science* 279, 1178–1181.

Moreno, H., Clavero, J. (2006) Geología del volcán Villarrica. Regiones de La Araucanía y de Los Lagos. Servicio Nacional de Geología y Minería, Carta Geológica Básica, No. 98, 35 pp., 1 mapa escala 1:50.000.

Newell, D.L., Jessup, M.J., Hilton, D.R., Shaw, C.A., Hughes, C.A. (2015) Mantle-derived helium in hot springs of the Cordillera Blanca, Peru: Implications for mantle-to-crust fluid transfer in a flat-slab subduction setting. *Chemical Geology* 417, 200–209.

Plank, T. (2005) Constraints from Thorium/Lanthanum on sediment recycling at subduction zones and the evolution of the continents. *Journal of Petrology* 46, 921–944.

Plank, T. (2014) 4.17 - The Chemical Composition of Subducting Sediments. In: Holland, H.D., Turekian, K.K. (Eds.) *Treatise on Geochemistry*. Second Edition, Elsevier, Oxford, 607–629.

Rivera, M., Martin, H., Le Pennec, J.L., Thouret, J.C., Gourgaud, A., Gerbe, M.C. (2017) Petro-geochemical constraints on the source and evolution of magmas at El Misti volcano (Peru). *Lithos* 268–271, 240–259.

Rivera, M., Thouret, J.C., Samaniego, P., Le Pennec, J.L. (2014) The 2006–2009 activity of the Ubinas volcano (Peru): Petrology of the 2006 eruptive products and insights into genesis of andesite magmas, magma recharge and plumbing system. *Journal of Volcanology and Geothermal Research* 270, 122–141.

Rizzo, A.L., Di Piazza, A., de Moor, J.M., Alvarado, G.E., Avard, G., Carapezza, M.L., Mora, M.M. (2016) Eruptive activity at Turrialba volcano (Costa Rica): Inferences from $^{3}He/^{4}He$ in fumarole gases and chemistry of the products ejected during 2014 and 2015. *Geochemistry, Geophysics, Geosystems* 17, 4478–4494.

Robidoux, P., Aiuppa, A., Rotolo, S.G., Rizzo, A.L., Hauri, E.H., Frezzotti, M.L. (2017) Volatile contents of mafic-to-intermediate magmas at San Cristóbal volcano in Nicaragua. *Lithos* 272–273, 147–163.

Robidoux, A.L. Rizzo, F. Aguilera, A. Aiuppa, M. Artale, M. Liuzzo, M. Nazzari, F.Z. (2020) Petrological and noble gas features of Lascar and Lastarria volcanoes (Chile): Inferences on plumbing systems and mantle characteristics. *Lithos* 370–371, 105615.

Samaniego, P., Rivera, M., Mariño, J., Guillou, H., Liorzou, C., Zerathe, S., Delgado, R., Valderrama, P., Scao, V. (2016) The eruptive chronology of the Ampato-Sabancaya volcanic complex (Southern Peru). *Journal of Volcanology and Geothermal Research* 323, 110–128.

Sancho, A. (2019) Rol e implicancias de los volátiles magmáticos en las condiciones pre-eruptivas de los centros eruptivos menores Caburgua y Chaillupén, Andes del Sur, Memoria entregada a la Universidad Mayor en cumplimiento de los requisitos para optar al Título de Geóloga. B.Sc. Thesis, Universidad Mayor, Escuela de Geología, Santiago, 137 pp.

Sarda, P., Staudacher, T., Allègre, C.J. (1988) Neon isotopes in submarine basalts. *Earth and Planetary Science Letters* 91, 73–88.

Simmons, S.F., Sawkins, F.J., Schlutter, D.J. (1987) Mantle-derived helium in two Peruvian hydrothermal ore deposits, *Nature* 329, 429–432.

Thouret, J.-C., Rivera, M., Gerbe, M.-C., Finizola, A., Fornari, M., Azur, G., Gonzales, K. (2005) Ubinas: the evolution of the historically most active volcano in southern Peru. *Bulletin of Volcanology* 67, 557–589.

Witter, J.B., Kress, V.C., Delmelle, P., Stix, J. (2004) Volatile degassing, petrology, and magma dynamics of the Villarrica Lava Lake, Southern Chile. *Journal of Volcanology and Geothermal Research* 134, 303–337.